# PEEK Oligomers as Physical Model Compounds for the Polymer. 4. Lamellar Microstructure and Chain Dynamics.

**O. Dupont,† A. M. Jonas,* B. Nysten, and R. Legras**

*Unité de Physique et de Chimie des Hauts Polymères, Université Catholique de Louvain, Place Croix du Sud, 1, 1348 Louvain-la-Neuve, Belgium*

**P. Adriaensens and J. Gelan**

*Div. Chem., Inst. Mat. Res., Gebouw D, Universitaire Campus, Limburgs Universitair Centrum, 3590 Diepenbeek, Belgium*

*Received July 12, 1999; Revised Manuscript Received November 4, 1999*

ABSTRACT: Crystals of monodisperse linear poly(oxy-1,4-phenyleneoxy-1,4-phenylenecarbonyl-1,4-phenylene) (PEEK) oligomers have been reinvestigated by wide-angle and small-angle X-ray scattering and atomic force microscopy (AFM). For the shorter oligomer investigated (containing six phenyl groups), a correlated packing of the chains is observed in the direction of the chain axis, with the formation of crystals being much thicker than the oligomer extended chain length. This results from the alignment of chain ends in planes, as revealed by AFM. A crystal structure is proposed for this oligomer, consistent with both AFM and X-ray diffractometry results. By contrast, the longer oligomer (containing 12 phenyl groups) presents a crystalline morphology consisting of stacks of atomically uncorrelated thin lamellar crystals, whose thicknesses are about the extended chain length computed for the oligomer. This is due to random staggering of the chains along their axes in the crystals, as suggested previously. CP/MAS $^{13}C$ solid-state NMR proton spin−lattice relaxation experiments reveal that these morphological differences induce variations in the chain dynamics of the oligomers and confirm that only the longer oligomer can be taken as a good model for a isolated crystal phase. From this study, reference values at room temperature are proposed for the specific mass of a perfect PEEK crystal [1.412(1) g·cm$^{-3}$] and for the proton spin−lattice relaxation time of such a crystal [3.6(2) s].

## Introduction

Poly(oxy-1,4-phenyleneoxy-1,4-phenylenecarbonyl-1,4-phenylene) (PEEK) (Figure 1) is a semicrystalline polymer with good mechanical properties, high-temperature stability and resistance to all common solvents. The crystalline structure of PEEK is well-known,[1−4] and no evidence for polymorphism has been found for this polymer. The crystal unit cell is orthorhombic (space group *Pbcn*) and contains two chains having a planar zigzag conformation (trans−trans conformation). By convention, **a** is the unit cell vector perpendicular to the zigzag plane (**b**−**c** planes) and **c** is the unit cell vector parallel to the chain axis direction. The tilt angle of the phenyl groups relative to (2 0 0) planes lies between 30 and 40°. Crystallographic studies all agree in considering ether and ketone bridges as crystallographically equivalent. Thus, the *c*-axis is only two-thirds of the polymer repeating unit. It has also been shown that unit cell dimensions are dependent on crystallization temperature.[5−8] They decrease with increasing crystallization temperature, suggesting better chain packing. This raises questions as to the limiting values of cell parameters for a perfect PEEK crystal and its associated crystalline density. It is one of the purposes of this paper to answer these questions, by considering the structure of PEEK monodisperse oligomers taken as physical model compounds for the polymer.

Reports on the synthesis and thermal properties of such oligomers, as well as preliminary structural information, have been previously published.[9,10] Several strictly monodisperse oligomers have been synthesized, differing in their chain ends (fluoroaryl ketone-ended and phenoxy-ended oligomers).[9] The extended chain lengths of the oligomers are comparable to the lamellar thickness of usual PEEK crystals. It was shown that the crystalline packing of the oligomers in the plane perpendicular to the chain axis direction is comparable with the packing observed for PEEK crystals.[10]

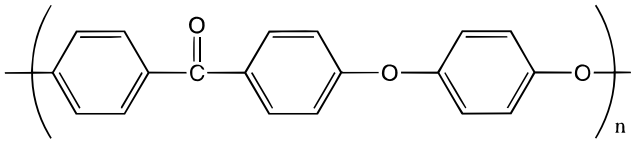


**Figure 1.** Repeat unit of PEEK.

In the present paper, a more complete analysis of the X-ray diffractograms of selected PEEK oligomers will be presented. Supplementary tools of data analysis will be used, like a modified Rietveld procedure developed for the characterization of wide-angle X-ray scattering (WAXS) patterns of PEEK.[11,12] Furthermore, the small-angle X-ray scattering (SAXS) patterns of these compounds will be revisited. Complementary information provided by atomic force microscopy (AFM) will also be used to help solving the structures of the crystals. Three oligomers of increasing length, having different WAXS patterns, have been selected for the present study (Table 1): a short phenoxy-ended oligomer containing 6 phenyls (labeled EEKEE), a long phenoxy-ended oligomer containing 12 phenyl groups (labeled EEK(EEK)$_2$EE), and a fluoroaryl ketone-ended oligomer of intermediate length containing 8 phenyl groups (labeled FK(EEK)$_2$F).

While the crystal structure of PEEK has been extensively studied, less information is available concerning

† Current address: UCB Chemicals S. A.; 33 rue d'Anderlecht; B1620 Drogenbos; Belgium.

10.1021/ma991116m CCC: $19.00 
Published on Web 12/31/1999

**Table 1. Nomenclature and Estimated Extended Chain Length of the Oligomers Used in This Study (Φ Stands for a Para-Substituted Phenyl Ring)**

| compound | nomenclature | extended length (Å) |
|---|---|---|
| ΦOΦOΦ(CO)ΦOΦOΦ | EEKEE | 31.0 |
| FΦ(CO)Φ(OΦOΦ(CO)Φ)$_2$F | FK(EEK)$_2$F | 41.9 |
| ΦOΦOΦ(CO)Φ(OΦOΦ(CO)Φ)$_2$OΦOΦ | EEK(EEK)$_2$EE | 60.4 |

amorphous regions of the polymer, and about interactions between amorphous and crystalline regions in the semicrystalline structure. Previous studies in the field have indicated significant differences between the properties of amorphous regions in semicrystalline samples and the properties of bulk amorphous PEEK. The following effects have been reported: a decrease of the heat capacity[13] and dielectric permittivity[14−16] of amorphous regions in semicrystalline samples vs pure amorphous PEEK, and an increase of the glass transition temperature in semicrystalline samples, which is correlated to the size of amorphous regions.[17,18] In turn, typical crystal properties such as thermal expansion have been shown to be partly controlled by the glassy or devitrified state of amorphous regions.[8] Many questions remain concerning these interactions between amorphous and crystalline regions. Yet, these questions are important since the nature of this coupling certainly governs the mechanical properties of the polymer.

To answer these questions, it is highly desirable to possess a standard sample, characteristic of the pure crystalline phase of the polymer with no coupling to amorphous regions. Then, the comparison of the properties of a semicrystalline polymer sample with those of the crystalline standard and of a pure amorphous sample may help to unravel coupling effects between amorphous and crystalline regions in the semicrystalline sample. In this respect, experimental techniques sensitive to chain dynamics are particularly interesting. Solid state nuclear magnetic resonance (NMR) is a technique able to characterize the dynamics of polymeric solids at a molecular level. At temperatures below the glass transition temperature ($T_g$), the phenomenon of spin diffusion is very efficient. Under these conditions, solid state NMR is very sensitive to the nanoscale morphology of semicrystalline polymers. In particular, the proton spin−lattice relaxation time $T_1$(H), spatially averaged over several tens of nanometers due to spin diffusion, is dependent on morphology. The $T_1$(H) value measured for a semicrystalline sample below $T_g$ should be a molar averaged value of the $T_1$(H) value of the amorphous fraction and the $T_1$(H) value of the crystal. Hence, obtaining information on the dynamic properties of amorphous regions from a determination of $T_1$(H)'s of semicrystalline PEEK samples is possible, provided one knows the $T_1$(H) value of PEEK crystals. In this paper, CP/MAS $^{13}$C solid-state NMR $T_1$(H) relaxation experiments on selected PEEK oligomers are presented. From these results and the former structural information, we decide which oligomer forms crystals that can be taken as good models for PEEK crystals in studies of chain dynamics. This is finally checked by performing a simple NMR measurement on one polymer sample and analyzing the data with the previous information.

## Experimental Section

The synthesis of PEEK monodisperse oligomers is described elsewhere.[9] The three oligomers selected are presented in Table 1, together with their labels for the present study. Except when stated otherwise, the recrystallized synthesis powders[10] were used without further thermal treatment.

PEEK (grade 150P, $M_n$ = 10 300 g/mol) was received from ICI. Glassy amorphous PEEK samples in the form of sheets (0.4 mm thickness) were prepared as described elsewhere.[8] A polymer sample was also cold-crystallized at 260 °C for 30 min for solid-state NMR experiments.

**WAXS** measurements were performed as previously described.[11] Acquisition conditions were slightly adapted from sample to sample. The data were corrected for absorption and variation of sampled volume with angle, and the Compton scattering was removed using Ruland's procedure.[19] The X-ray data for the longer oligomer (EEK(EEKEE)$_2$EE) were analyzed by a modified Rietveld procedure described elsewhere.[11,12] For the shorter oligomer, the data were simply analyzed using a full profile fitting procedure where each crystalline reflection is fitted by the convolution of a Voigt function[20] with an instrumental aberration function.[21−23] A complete description of the instrumental aberration function used in the present study can be found in a previous paper.[11]

**SAXS** patterns were recorded in an evacuated Kratky camera (slit collimation) mounted on a Siemens rotating anode generator (Ni-filtered Cu Kα radiation, 40 kV/300 mA). A position-sensitive proportional counter (Braun) was used to record the diffraction patterns. After correction for parasitic scattering and background subtraction, the recorded curves were desmeared using a variant of Glatter's algorithm.[24] The curves were finally Lorentz-corrected. One-dimensional correlation functions were computed from SAXS intensities by performing a Fourier transform. For sample EEKEE, the SAXS and WAXS data were merged into a single set, as overlapping reflections existed in both ranges. In this case, the one-dimensional correlation function was computed from all (00*l*) reflections.

**AFM** experiments were performed on thin oligomer films (about 10 $\mu$m) deposited onto microscope glass slides, and crystallized isothermally from the melt at different temperatures. Error images were obtained under ambient conditions in contact mode with a AutoProbe CP system (Park Scientific Instruments, Sunnyvale, CA), using a 5 $\mu$m scanner. $Si_3N_4$ cantilevers (of stiffness about 0.1 N m$^{-1}$) with integrated pyramidal tips were used.

All solid-state cross-polarization magic-angle spinning **$^{13}$C−CP/MAS NMR** spectra were recorded at room temperature on a Varian XL-200 spectrometer at 50.3 MHz with a spectral width of 18500 Hz. MAS was performed at 7 kHz using $Si_3N_4$ rotors. The magic angle was set with KBr, while the Hartman−Hahn conditions were adjusted using the aromatic resonance of hexamethylbenzene. The chemical shift of this resonance (132.1 ppm) was also employed to calibrate the chemical shift scale toward tetramethylsilane (TMS). To minimize the effect of long-term drift, the NMR relaxation experiments were interleaved block averaged with 8 acquisitions per block. A $\pi/2$ pulse width of 8.4 $\mu$s was used yielding a spin lock field of 30 kHz during cross-polarization. High power decoupling (45 kHz) was applied during the acquisition time (20 ms). $T_1$(H) relaxation times were measured by means of the inversion recovery method using about 400 spectrum accumulations for each evolution time and fixed contact times of 1.5 ms and 3 ms for the polymer samples and the oligomers, respectively. A preparation delay of 5 times the $T_1$(H) value was respected (varying from 5 to 120 s for the polymers and oligomers, respectively). The evolution times were on the order of 0.01−7 s for polymers and 0.2−130 s for oligomers.

## Results and Discussion

**Structure of EEKEE.** The X-ray diffractogram (combined WAXS and SAXS patterns) of the shorter oligomer is presented in parts a and b of Figure 2. Compared to the diffractogram of the polymer sample (Figure 2d), the pattern of this oligomer presents a series of additional reflections. As these cannot be indexed in terms of the usual orthorhombic unit cell of

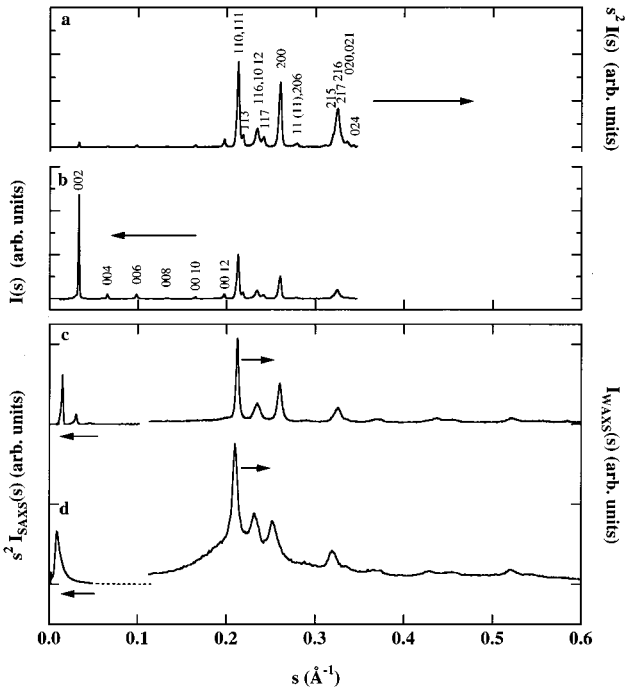


**Figure 2.** X-ray diffractograms: (a) oligomer EEKEE, Lorentz-corrected (merged WAXS and SAXS data); (b) oligomer EEKEE (merged WAXS and SAXS data); (c) oligomer EEK(EEK)$_2$EE (Lorentz-corrected SAXS, left; WAXS, right); (d) PEEK crystallized at 260 °C for 30 min (Lorentz-corrected SAXS, left; WAXS, right).

the polymer, an other unit cell was considered. A complete indexing can be successfully performed in terms of a larger orthorhombic unit cell with values of *a* and *b* similar to those of the polymer and *c* about twice the estimated extended length of the oligomer. From a full profile fitting procedure, the following values were obtained for the unit cell parameters: $a = 7.6554(3)$ Å; $b = 5.9092(5)$ Å; $c = 60.53(7)$ Å. From the fit, the squared structure factors ($|F_{exp}|^2$) of about 15 reflections were also obtained (Table 3).

To help solve the structure of EEKEE crystals, AFM experiments were performed. Images resolved at the atomic scale could be easily obtained for these crystals. Figure 3 (left) presents one of the best images obtained, with its associated power spectral density (Figure 3, center). By retaining 11 pairs of spots from the power spectral density, a high-resolution filtered image was obtained (Figure 3, right). This image coincides with the lateral packing of terminal phenyls of EEKEE chains that one would expect if the oligomers adopt in the crystals a conformation similar to the polymer in its crystals and if the oligomer chain ends all align in planes to form the crystal surface. This is shown more explicitely in Figure 4, where a view of the expected packing of terminal phenyl groups is shown (plane group: *pg*) and compared to a zoomed portion of the filtered AFM image. As clearly appears, the AFM is essentially sensitive to the topmost atoms of the chain ends, the hydrogen atom at the apex of the phenyls, and one of the hydrogen atoms in the *ortho* position with reference to the apex hydrogen. This second H atom is located only about 0.4 Å lower than the H atom at the apex, because of the torsion angle of the phenyls (~35° with respect to the *b*−*c* plane) and of the valence angle of ether links in the chain (~120°). The center part of the top image in Figure 4 presents only the expected packing for these two upper H atoms. The similarity with the AFM data is rather rewarding.

From this extra knowledge, and from the observation of extinction of all $(0,0,2n + 1)$ reflections, a crystal structure could be found and refined, consistent with both the AFM data and the measured X-ray structure factors (space group *Pbcn*; Figure 5, Tables 2 and 3). The unit cell contains four molecules, packed by two in layers; molecules in the second layer are related to molecules in the first layer by a $2_1$ screw axis (Figure 5). Chains adopt a planar zigzag conformation similar to the polymer in its crystals, with the phenyls regularly tilted in opposite directions by 34−37° about the *b*−*c* plane. The bridge (ether and ketone) angles are about 126°, which is similar to the values found for the polymer.[4,11,12] As pointed out in other studies of shorter oligomers of the aryl−ether−ketone family,[25] these values may be slightly erroneous due to the neglect of distortions of phenyl rings in our refinement procedure. The location of the $2_1$ screw axis is such that the lowest H atoms of the second layer (black spots in the right part of the top image in Figure 4) fit in the grooves left on the top surface of the first layer. The existence of these grooves cannot be missed from the examination of the AFM image (bottom of Figure 4).

The fact that EEKEE chain ends pack into planes results in the formation of molecular crystals with correlations in atomic positions extending over large distances in the *c*-axis direction. This is the origin of the supplementary WAXS reflections as compared to the polymer crystals. These long-range correlations are also evident from a consideration of the normalized one-dimensional correlation function computed from (00*l*) reflections (Figure 6a). An oscillation with a period of about 5 Å, corresponding to the repetition of the phenyl groups along the chains and from layer to layer, can be detected over distances larger than 600 Å. This clearly confirms that atomic positions are highly correlated in the *c*-axis direction.

**Structure of EEK(EEK)$_2$EE.** The WAXS and SAXS patterns of the longest oligomer are presented in Figure 2c, together with those of the polymer (Figure 2d). The oligomer and polymer patterns are now almost identical, with the exception of the SAXS range where significant differences can be noticed. In the WAXS range, the differences between polymer and oligomer consist only in the presence of an amorphous halo for the semicrystalline polymer. Hence, contrary to the previous short oligomer, the WAXS data can be indexed with the usual unit cell of PEEK. We thus performed a whole pattern refinement procedure for this sample, similar to the procedure developed for the polymer.[11,12] This procedure gives access to structural information such as unit cell parameters (*a*, *b*, *c*), average quadratic atomic displacements ($\langle u_a^2 \rangle$), $\langle u_b^2 \rangle$, $\langle u_c^2 \rangle$), paracrystalline factors in three directions ($\Delta a/a$, $\Delta b/b$, $\Delta c/c$), and estimations for the crystal dimensions in three directions (*A*, *B*, *C*). The results of this procedure are presented in Table 4. Considering the values of the criteria of goodness of fit, the model curve designed to fit the diffraction pattern from lamellae of semicrystalline PEEK can be considered to be accurate enough to represent the oligomer scattering. The values of the unit cell parameters $b = 5.9326(6)$ Å and $c = 9.954(5)$ Å are in the same range as those determined for various semicrystalline PEEK samples[11,12] ($b = 5.89-5.93$ Å; $c = 9.96-9.99$ Å). However, the unit cell parameter *a* is significantly lower

**Table 2. Main Parameters Used to Compute the Structure Factors of EEKEE Crystals**

| parameter | value | status during fit |
|---|---|---|
| C=C length in phenyls (Å) | 1.395 | held constant |
| C−H length in phenyls (Å) | 1.08 | held constant |
| C−O length in ether bridges (Å) | 1.36 | held constant |
| C−(CO) length in ketone bridges (Å) | 1.47 | held constant |
| C=O length (Å) | 1.23 | held constant |
| bridge angle (ether and ketone) (deg) | 126.19 | held constant |
| torsion angle of phenyl groups, relative to (*b*, *c*) planes (except terminal phenyls) (deg) | 33.9 | fitted |
| torsion angle of terminal phenyl groups, relative to (*b*,c) planes (deg) | 36.6 | fitted |
| shift of second layer relative to the first in *b* direction (internal reference, Å) | 3.83 | fitted |
| shift of second layer relative to the first in *a* direction (internal reference, Å) | −0.77 | fitted |
| thermal disorder parameter[27] (Å$^2$) | 5.15 | fitted |
| *r* parameter of the March−Dollase preferred orientation function[26] | 0.936 | fitted |

**Table 3. Experimental and Computed Squared Structure Factors for EEKEE Crystals[c]**

| *hkl* | | $\|F_{calc}\|^2$ [a] | $\|F_{exp}\|^2$ [b] |
|---|---|---|---|
| 002 | | $9.66 \times 10^3$ | $1.23 \times 10^4$ |
| 004 | | $2.26 \times 10^3$ | $2.84 \times 10^3$ |
| 006 | | $9.11 \times 10^3$ | $9.57 \times 10^3$ |
| 008 | | $2.56 \times 10^3$ | $3.11 \times 10^3$ |
| 00(10) | | $9.24 \times 10^3$ | $8.12 \times 10^3$ |
| 00(12) | | $4.16 \times 10^4$ | $4.16 \times 10^4$ |
| 110 | | $1.17 \times 10^5$ | |
| 111 | | $3.58 \times 10^5$ | |
| | sum | $4.75 \times 10^5$ | $4.97 \times 10^5$ |
| 113 | | $7.77 \times 10^4$ | $4.71 \times 10^4$ |
| 116 | | $1.71 \times 10^5$ | |
| 10(12) | | $4.06 \times 10^4$ | |
| | sum | $2.12 \times 10^5$ | $1.81 \times 10^5$ |
| 117 | | $1.06 \times 10^5$ | $6.33 \times 10^4$ |
| 200 | | $4.44 \times 10^5$ | $4.48 \times 10^5$ |
| 11(11) | | $2.90 \times 10^4$ | |
| 206 | | $5.75 \times 10^3$ | |
| | sum | $3.48 \times 10^4$ | $3.80 \times 10^4$ |
| 215 | | $1.77 \times 10^4$ | |
| 216 | | $3.75 \times 10^5$ | |
| 217 | | $5.01 \times 10^4$ | $4.68 \times 10^5$ |
| | sum | $4.43 \times 10^5$ | |
| 020 | | $1.30 \times 10^4$ | |
| 021 | | $2.40 \times 10^4$ | |
| | sum | $3.70 \times 10^4$ | $4.55 \times 10^4$ |

[a] Computed squared structure factors. [b] Experimental squared structure factors. [c] The computed structure factors are obtained using the structural data in Table 2. The fit converged toward a residual index[27] $R = 0.081$

for the oligomer ($a = 7.6563(8)$ Å) than for the polymer ($a = 7.74-7.83$ Å). Moreover, the parameters related to the lattice distortions in the a direction are either comparable (paracrystalline factor, $\Delta a/a$) or much smaller (mean quadratic atomic displacement, $\langle u_a^2 \rangle$) than the lowest values observed for the polymer samples.[11,12] This set of observations indicates that the packing of the planes containing the zigzag backbones of the molecular chains (*b*−*c* planes) is closer and more regular in the oligomer than in the polymer. It has been observed[11,12] that, for PEEK polymer crystals, the defects in the crystalline lattice occur mainly perpendicularly to *b*−*c* planes. For samples crystallized at increasingly higher temperatures, the lattice reorganizes with a closer packing of the zigzag planes without much variation inside these planes. This suggests that the crystalline lattice of the oligomer can be considered to be close to the "ideal" crystalline packing of PEEK chains.

The lamellar thickness C of the oligomer (=60.0(7) Å) is comparable to the thickness of lamellae in semicrystalline PEEK samples, and is remarkably close to the value of the estimated chain length for this compound (60.4 Å). This indicates that, contrary to the shorter oligomer, EEK(EEK)$_2$EE crystallizes into thin lamellar crystals, with no correlation between atom positions in neighboring crystals, i.e., no register between two successive crystals. The SAXS pattern of the oligomer confirms this conclusion. Indeed, the one-dimensional correlation function computed from the "layer lines" (Figure 6c) reveals only a monoperiodic variation with no sign of correlation between successive phenyl groups as for oligomer EEKEE. The only correlations found are between the centers of mass of successive crystals, which stack relatively regularly into larger assemblies.

The period of the oscillations in the correlation function (65 Å) is significantly larger than either the lamellar thickness computed by WAXS or the estimated extended chain length. Hence, lamellar crystals of EEK(EEK)$_2$EE are separated by gaps of about 5 Å average thickness that destroy correlations in atomic positions in the *c*-direction. These regions most probably arise from the existence of staggered chains, i.e., some chains ends protrude from the crystal by one phenyl group as hypothesized previously.[10] This is indirectly confirmed by AFM experiments. Because of the typical tip radius (30−50 nm), high resolution images can only be obtained by AFM on smooth surfaces, regular at the atomic scale. As it was not possible to obtain atomic resolution images on the crystals of EEK(EEKEE)$_2$EE, while this was possible for EEKEE crystals, one can safely conclude that the crystal surfaces are atomically much rougher and disordered for EEK(EEKEE)$_2$EE.

The gaps created between two successive lamellae by the random staggering of chains may not be considered as truly amorphous but are sufficient to effectively isolate each lamella from its neighbors. The fact that random staggering of the chains is possible for these crystals also supports the hypothesis that the perturbations of crystal structure by the chain ends is negligible. Hence, crystals of the EEK(EEK)$_2$EE oligomer can be considered as ideal isolated PEEK crystals without either long-range correlations between successive crystals, or coupling to a disordered amorphous region. Such crystals have a specific mass of 1.412(1) g·cm$^{-3}$.

**Structure of FK(EEK)$_2$F.** We also studied this oligomer of intermediate length with different chain ends. We found that its behavior is intermediate between the two extremes EEKEE and EEK(EEK)$_2$EE, with partial correlations in atom positions extending from layers to layers (Figure 6b). More information about the structure of this oligomer will not be reported in the present paper.

**NMR Studies.** CP/MAS $^{13}$C solid-state NMR has been applied to the three oligomers, to determine their relaxation time $T_1$(H). These values are reported in Table 5. It appears that the $T_1$(H) relaxation times of the oligomers are very different from each other. This confirms that all these compounds cannot be taken as

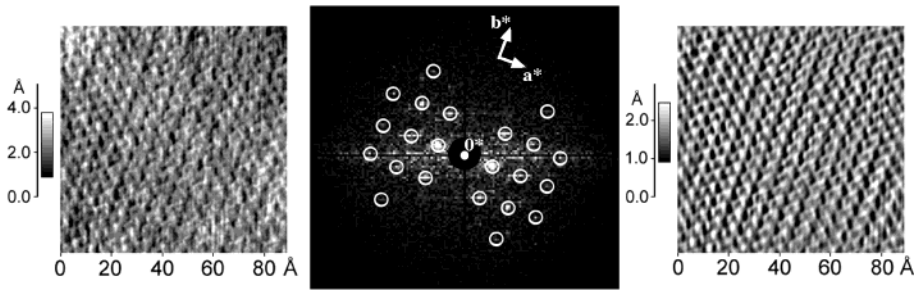


**Figure 3.** (Left): Unfiltered AFM image of the surface of EEKEE crystals. (Center): Power spectral density of the unfiltered image; circled spots are reflections used for filtering. (Right): Filtered image.

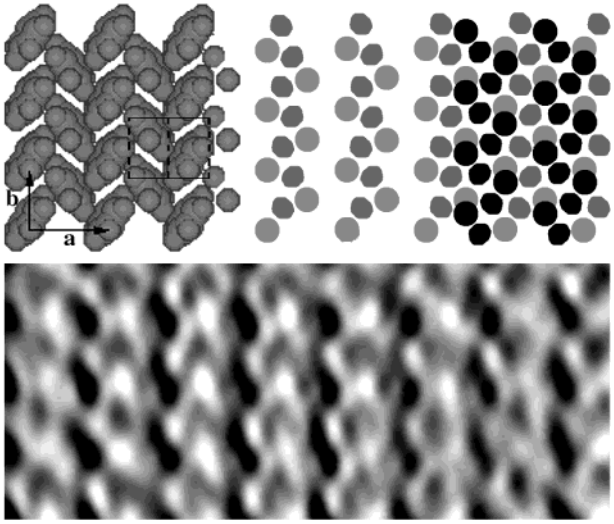


**Figure 4.** (Top): Packing of terminal phenyls in EEKEE crystals. The center part of the image only displays the two topmost hydrogen atoms, while the right part of the image shows in black the locations of the corresponding lowest hydrogen atoms of the next EEKEE layer. (Bottom): Magnified view of the filtered AFM image, where the typical "knitted" arrangement of phenyl groups on (002) faces is clearly evident.

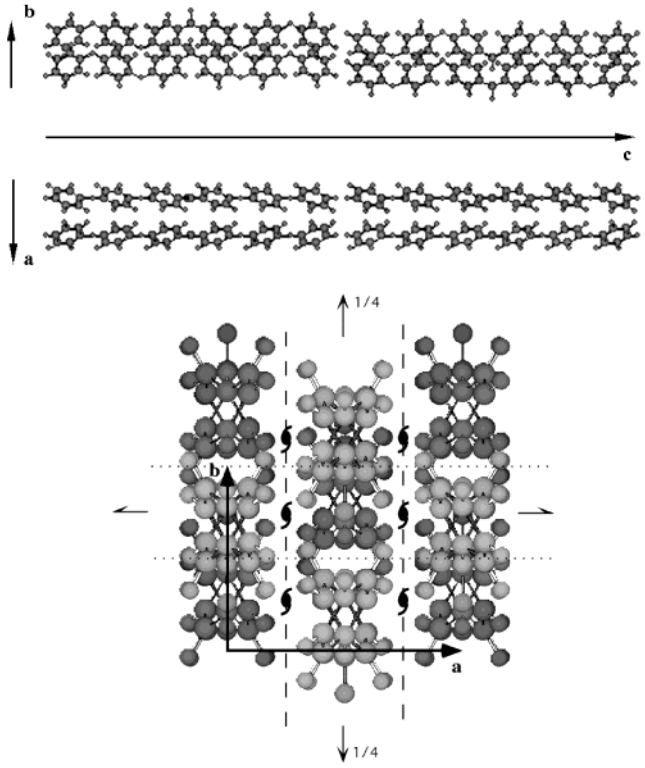


**Figure 5.** (Top): Projections on (*b*,*c*) and (*a*,*c*) planes of the four chains of the unit cell of EEKEE crystals. (Bottom): Projection on the (*a*,*b*) plane of the unit cell of EEKEE crystals, showing the main symmetry elements (space group *Pbcn*).

good models for pure PEEK polymer crystals. Clearly, the morphological differences between oligomer crystals described above induce large variations in the measured relaxation time $T_1$(H). This parameter is apparently sensitive to differences in the degree of correlation between successive lamellar crystallites: as the interlamellar atomic correlations vanish from EEKEE to EEK(EEK)$_2$EE, $T_1$(H) also decreases by about an order of magnitude (from 23.2 to 3.56 s).

To check our previous conclusion that crystals of EEK(EEK)$_2$EE should be good models for the crystalline phase of semicrystalline PEEK, we have determined the $T_1$(H) relaxation time of a semicrystalline PEEK sample isothermally cold-crystallized at 260 °C during 30 min and of an amorphous (quenched) PEEK sample (Table 5). A single $T_1$(H) value (monoexponential fit), similar for all $^{13}$C resonances in the spectrum, is obtained for the semicrystalline PEEK sample. This is due to the fact that the mobility of the chain segments below the glass transition temperature is very low in amorphous as well as in crystalline regions, allowing complete spin diffusion.

Under this condition, $T_1$(H), being sensitive to Larmor frequencies (around 200 MHz), is averaged out over a rather large distance of several tens of nanometers. The *maximum* diffusive path length, $L_D$ over which proton−proton spin diffusion can occur can be approximated by $L_D = (6DT_1(H))^{1/2}$, where $D$ is the spin diffusion coefficient ($\sim 10^{-16}$ m$^2$/s for rigid solids). Under conditions of spin diffusion, the relaxation time of a semicrystalline sample ($T$) can be written as

$$\frac{1}{T} = \psi_c \frac{1}{T_c} + (1 - \psi_c)\frac{1}{T_a} \qquad (1)$$

where $\psi_c$ is the crystallinity by weight, and $T_c$ and $T_a$ are, respectively, the relaxation times associated with the crystalline lamellae and with the amorphous regions.

A strategy to validate this formula is to compare experimental values of $T$ with values computed by eq 1, with $T_c$ and $T_a$ set equal to the relaxation times of the PEEK crystal and of a fully amorphous PEEK sample, respectively. $T_a$ was determined on a pure amorphous PEEK sample to be 1.40 s (Table 5).

The experimental and the computed (eq 1) values of the relaxation times $T_1$(H) of the semicrystalline sample of PEEK ($\psi_c$ = 25.5% as previously determined[11]) are reported in Table 5. Considering the values of $T_1$(H), it appears that $T_1$(H) computed with $T_c$ selected as the

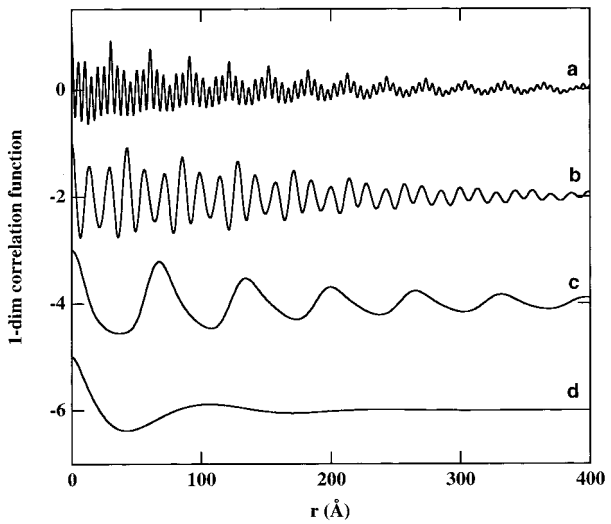


**Figure 6.** Normalized one-dimensional correlation functions: (a) EEKEE, calculated from the merged SAXS and WAXS patterns (00*l* layer lines); (b) FK(EEK)$_2$F (SAXS data only); (c) EEK(EEK)$_2$E (SAXS data only); (d) PEEK crystallized at 260 °C for 30 min (SAXS data only). For clarity, curves are regularly shifted downward by increments of 2.

**Table 4. List of the Refined Parameters for the Structure of EEK(EEK)$_2$EE Oligomer Crystals**[a]

| parameter | refined value |
|---|---|
| $\psi$ (deg) | 0 |
| $a$ (Å) | 7.6563(8)[d] |
| $b$ (Å) | 5.9326(6) |
| $c$ (Å) | 9.954(5) |
| $A$ (Å) | 674(103) |
| $B$ (Å) | 321(11) |
| $C$ (Å) | 60.0(7) |
| $\Delta a/a$ (%) | 3.24(2) |
| $\Delta b/b$ (%) | 2.9(1) |
| $\Delta c/c$ (%) | 0.01(9) |
| $\langle u_a^2 \rangle$ (Å$^2$) | 0.003(4) |
| $\langle u_b^2 \rangle$ (Å$^2$) | 0.01(1) |
| $\langle u_c^2 \rangle$ (Å$^2$) | 0.00(1) |
| $\chi^2/N$[b] | 4.40 |
| Rp[c] | 0.084 |
| Rwp[c] | 0.118 |

[a] Definition of the parameters: $\psi$, tilt of the chain axis vs the normal to the basal plane of the lamella; $a$, $b$, and $c$, unit cell parameters; $A$, $B$, and $C$, lamellar dimensions ($C$ is the lamellar thickness); $\Delta a/a$, $\Delta b/b$, and $\Delta c/c$, paracrystalline factors; $\langle u_a^2 \rangle$, $\langle u_b^2 \rangle$, and $\langle u_c^2 \rangle$, mean quadratic atomic displacements (for a complete definition of these parameters, see ref 11). [b] $N$ is the number of experimental points in each diffractogram. [c] Rp and Rwp are usual numerical criteria for the goodness of fit (for a complete definition and discussion, see[11]) [d] The estimated standard deviations indicated in parentheses are those resulting from the diagonal terms of the inverted covariance matrix and are, most probably, underestimated (for a complete discussion see ref 11).

relaxation time of EEK(EEK)$_2$EE crystals is very close to the experimental value of $T_1$(H) for the semicrystalline sample ($\Delta < 2.5\%$). This is in complete agreement with expectations based on structural data and indicates that absence of atomic correlations between two successive lamellae is a prerequisite to the determination, from oligomer crystals, of meaningful reference values of $T_1$(H) for polymer crystals.

## Conclusions

We have reinvestigated by WAXS, SAXS, and AFM the structure of three monodisperse PEEK oligomers. A structure is proposed for the shorter EEKEE oligomer, consistent with both X-ray diffraction and high-resolution AFM images. The main feature of this structure is the existence of a register between successive layers of crystallized oligomers, giving rise to a supercell with atomic correlations existing between distant layers. For the longer oligomer (EEK(EEK)$_2$EE), however, atomic correlations between successive layers are destroyed, due to random staggering of the chains in the chain axis direction. This effectively isolates each crystal from its neighbors and indicates that chain ends may be considered as a minor structural perturbation for these crystals. Considering the fact that crystal thicknesses for this oligomer are in the range of thicknesses found for usual PEEK (polymer) crystals, one concludes that the density of EEK(EEK)$_2$EE [1.412(1) g·cm$^{-3}$] should be a good reference value for a PEEK ideal crystal without connections to amorphous regions.

**Table 5. CP/MAS $^{13}$C Solid State NMR Proton Spin−Lattice Relaxation Times ($T_1$(H)) of PEEK Oligomers and Two PEEK Samples**

| | $T_1$(H) (s) |
|---|---|
| PEEK oligomers | |
| EEKEE | 23.2 ± 0.5 |
| FK(EEK)$_2$F | 6.07 ± 0.3 |
| EEK(EEK)$_2$EE | 3.56 ± 0.2 |
| amorphous PEEK | 1.40 ± 0.03 |
| PEEK crystallized for 30 min at 260 °C | |
| experimental value | 1.61 ± 0.03 |
| computed value with $T_c$[a] | |
| $T_c$, EEKEE | 1.84 |
| $T_c$, FK(EEK)$_2$F | 1.74 |
| $T_c$, EEK(EEK)$_2$EE | 1.65 |

[a] See text (eq 1).

CP/MAS $^{13}$C solid-state NMR study also confirms the usefulness of oligomer EEK(EEK)$_2$EE as model compound for PEEK crystals. The absence of atomic correlations between successive crystals is apparently a requirement to obtain $T_1$(H) values for oligomer crystals that may be taken as typical for polymer crystals. For PEEK semicrystalline samples, we thus found that the $T_1$(H) value of crystalline lamellae can be taken as equal to the $T_1$(H) value of EEK(EEK)$_2$EE crystals [3.6(2) s at room temperature], which is significantly larger than the 1.4 s found for the $T_1$(H) of amorphous PEEK.

**Acknowledgment.** We acknowledge fruitful discussions with Profs. D. Ivanov and P. Damman. Financial support for this work was partly provided by the "Fonds pour la formation à la Recherche dans l'Industrie et dans l'Agriculture" (FRIA) and by the "Belgian National Fund for Scientific Research" (FNRS). The NMR research was executed in the framework of the IUAP (Interuniversitaire Attrakiepolen), financed by the Belgium Government (Diensten van de Eerste Minister-Federale diensten voor wetenschappelijke, technische en culturele aangelegenheden). Bernard Nysten is Research Associate of the FNRS.

## References and Notes

(1) Hay, J. N.; Kemmish, D. J.; Langford, J. I.; Rae, A. I. M. *Polym. Commun.* **1984**, *25*, 175.
(2) Fratini, A. V.; Cross, E. M.; Whitaker, R. B.; Adams, W. W. *Polymer* **1986**, *27*, 861.
(3) Hay, J. N.; Langford, J. I.; Lloyd, J. R. *Polymer* **1989**, *30*, 489.
(4) Iannelli, P. *Macromolecules* **1993**, *26*, 2309.
(5) Wakelyn, N. T. *J. Polym Sci. C, Polym. Lett.* **1987**, *25*, 25.
(6) Hay, J. N.; Langford, J. I.; Lloyd, J. R. *Polymer* **1989**, *30*, 489.
(7) Deslandes, Y.; Alva Rosa, E. *Polym. Commun.* **1990**, *31*, 269.

(8) Jonas, A. M.; Russell, T. P.; Yoon, D. Y. *Macromolecules* **1995**, *28*, 8491.
(9) Jonas, A. M.; Devaux, J.; Legras, R. *Macromolecules* **1992**, *25*, 5841.
(10) Jonas, A. M.; Legras, R.; Scherrenberg, R.; Reynaers, H. *Macromolecules* **1993**, *26*, 526.
(11) Dupont, O.; Jonas, A. M.; Legras, R. *J. Appl. Crystallogr.* **1997**, *30*, 921.
(12) Dupont, O.; Ivanov, D. A.; Jonas, A. M.; Legras, R. *J. Appl. Crystallogr* **1999**, *32*, 497.
(13) Cheng, S. Z. D.; Cao, M.-Y.; Wunderlich, B. *Macromolecules* **1986**, *19*, 1868.
(14) Kalika, D. S.; Krishnaswamy, R. K. *Macromolecules* **1993**, *26*, 4252.
(15) Cebe, P.; Huo, P. P. *Thermochim. Acta* **1994**, *238*, 229.
(16) Huo, P.; Cebe, P. *Macromolecules* **1992**, *25*, 902.
(17) Jonas, A. M.; Legras, R. *Macromolecules* **1993**, *26*, 813.
(18) Kalika, D. S.; Gibson, D. G.; Quiram, D. J.; Register, R. A. *J. Polym. Sci., Part B: Polym. Phys.* **1998**, *36*, 65.
(19) Ruland, W. *Br. J. Appl. Phys.* **1964**, *15*, 1301.
(20) Langford, J. I. *J. Appl. Crystallogr.* **1978**, *11*, 10.
(21) Wilson, A. J. C. In *Mathematical theory of X-ray powder diffractometry*; Parrish, W., Ed.; Philips technical library, Centrex publishing company: Eindhoven, The Netherlands, 1963.
(22) Klug, H. P.; Alexander, L. E. *X-ray diffraction procedures for polycrystalline and amorphous materials*; Wiley Interscience: New York, 1974.
(23) Cheary, R. W.; Coelho, A. *J. Appl. Crystallogr.* **1992**, *25*, 109.
(24) Glatter, O. *J. Appl. Crystallogr.* **1974**, *7*, 147.
(25) Colquhoun, H. M.; O'Mahoney, C. A.; Williams, D. J. *Polymer* **1993**, *34*, 218.
(26) Hill, R. J. In *The Rietveld Method;* Young, R. A., Ed.; International Union of Crystallography, Oxford University Press: Oxford, England, 1995; pp 61−101.
(27) Stout, G. H.; Jensen, L. H. *X-ray structure determination. A practical guide*, 2nd ed.; J. Wiley & Sons: New York, 1989.

MA991116M